



Factors affecting the retention of Cs⁺ primary ions in Si

P.A.W. van der Heide*, C. Lupu, A. Kutana, J.W. Rabalais

*Center for Materials Characterization (CMC), Chemistry Department, University of Houston,
136 Fleming Building, Houston, TX 77204-5003, USA*

Available online 30 April 2004

Abstract

X-ray photo-electron spectroscopy (XPS), Rutherford backscattering spectroscopy (RBS) along with MARLOWE and TRIM computer simulations were used to study the retention of Cs⁺ primary ions in Si substrates during sputtering. Cs concentrations were found to depend on (a) primary ion energy, (b) primary ion incidence angle, and (c) sputtering time (within the transient region). With the exception of the XPS and RBS data collected as a function of Cs⁺ impact energy, Cs concentration variations, $\Delta[\text{Cs}]$, appear to correlate with sputter yield variations, ΔSY , via $\Delta[\text{Cs}] \propto 1/(\Delta\text{SY} + 1)$. Computer simulations reveal variations in Cs⁺ scattering with impact energy, etc. This and/or self sputtering may explain the inconsistencies noted with impact energy. © 2004 Elsevier B.V. All rights reserved.

Keywords: SIMS; Cesium implantation; Silicon

1. Introduction

Secondary ion mass spectrometry (SIMS) is used extensively in the semiconductor industry for relaying information on dopant distributions. One of the reasons lies in its high sensitivity to specific elements, i.e., ppb levels are detectable. This stems, in part, from the use of chemically active primary ions since these strongly affect (up to $10^4\times$) the secondary ion yield. This arises from the small percentage of the primary ions that remain implanted in the substrate during sputtering (these affect the electronic structure and thus the ionization/neutralization probabilities of the resulting secondary ions). As a result, Cs⁺ is the most popular primary ion beam for analyzing distributions of *n* type dopants.

Any variation in the Cs concentration will strongly affect secondary ion yields. Indeed, this partially

explains the transient effects noted in SMIS. Since steady state Cs concentrations represent a state in which the amount of Cs implanted equals the amount of Cs sputtered, the steady state concentration will depend primarily on the Cs⁺ projectile range and the sputter rate of the substrate. Indeed, the Cs concentration, $[\text{Cs}]$, has been shown to follow the sputter yield, SY, via $\Delta[\text{Cs}] \propto 1/(\Delta\text{SY} + 1)$ but only under specific conditions [1–3]. The purpose of this study is to analyze the applicability of this relation over a wider range of conditions. Cs concentration variations were followed using X-ray photo electron spectroscopy (XPS) and Rutherford backscattering spectroscopy (RBS). Sputter rates and Cs⁺ scattering coefficients were derived via computer simulation.

2. Experimental

Samples comprised of Si(1 0 0) wafers terminated with a 0.9 nm native oxide. The native oxide thickness

* Corresponding author. Tel.: +1-713-743-2582,
fax: +1-713-743-2787.
E-mail address: pvanderheide@uh.edu (P.A.W. van der Heide).

was defined via XPS by a procedure outlined elsewhere [4].

Sputtering was carried out on a Physical Electronics 6600 quadrupole SIMS instrument using Cs^+ primary ions at incident angles from 40 to 80° with respect to the sample normal and impact energies from 1.0 to 5.0 keV. This was rastered over areas from $400\ \mu\text{m} \times 400\ \mu\text{m}$ to $2000\ \mu\text{m} \times 2000\ \mu\text{m}$ (this large area was required by RBS). Sputtering was terminated well after steady state secondary ion signals were observed. To minimize oxidation of the crater base regions, samples were transferred between SIMS and XPS instruments via a vacuum transfer device. Since this could not be used with the RBS instrument, air exposure was minimized.

XPS measurements were carried out on a Physical Electronics 5700 (XPS) instrument using a monochromatic Al $K\alpha$ X-ray source (1486.6 eV) operated at 350 W. Photo-emissions were collected at a takeoff angle of 45° from an area of $175\ \mu\text{m}$ in diameter, centered in the middle of the SIMS crater base regions. RBS measurements were carried out using a 30 nA, 2.06 MeV He^+ beam with a spot size of $1500\ \mu\text{m}$ in diameter. Again, this was centered in the middle of the enlarged SIMS crater base regions. The detector angle was set at 165° .

Sputter yields and Cs scattering coefficients were derived via the TRIM and MARLOWE computer simulations, respectively. An amorphous surface was simulated since sputtering induces the amorphization of Si. TRIM assumes this, while MARLOWE, in which a Moliere potential with a Firsov screening length was used [5], requires random rotation of the sample.

3. Results

Shown in Fig. 1(a) are the experimentally derived Cs concentrations as a function of Cs^+ primary ion incident angle (energy fixed at 1 keV). The XPS and RBS data are plotted on the left and right ordinate, respectively. These show the retained Cs concentration to decrease as the incidence angle is increased. Cs concentrations derived from the sputter yield relation are shown in the inset of Fig. 1(a) using both simulated and experimentally derived sputter yields. On the whole, these reveal a similar trend to each other

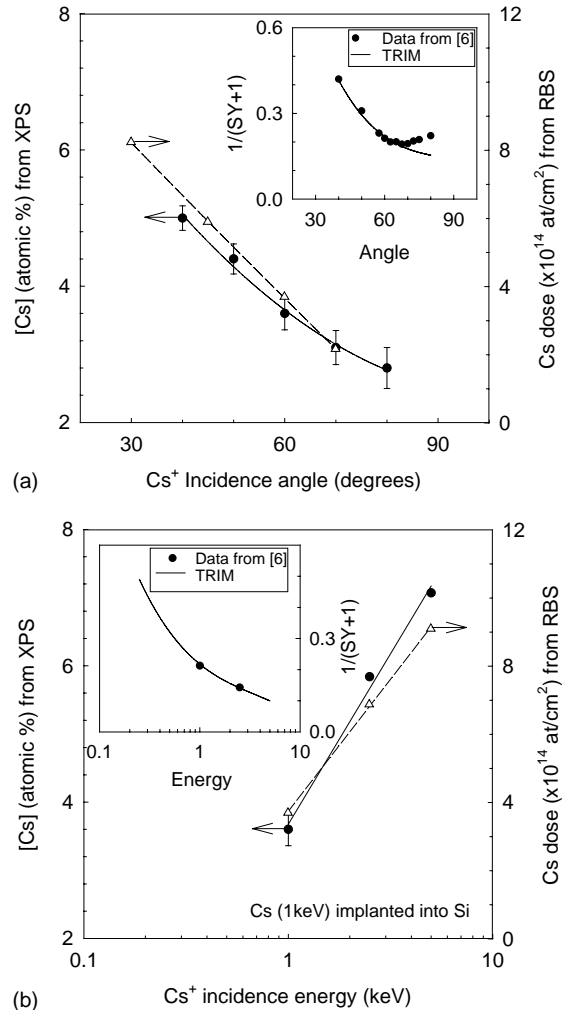


Fig. 1. XPS and RBS defined Cs concentrations as a function of (a) Cs^+ incident angle at 1 keV impact and (b) Cs^+ impact energy at 60° incidence. In the insets the Cs concentrations derived via the sputter yield relation using both experimentally derived [6] and simulated sputter yields are shown.

and to those derived via XPS and RBS. The deviations noted at higher incidence angles in the inset of Fig. 1(a) have been ascribed to the increased sputter rates associated with surface roughening [6].

Shown in Fig. 1(b) are the experimentally derived Cs concentrations as a function of Cs^+ primary ion impact energy (angle fixed at 60°). These show the retained Cs concentration to increase with increasing impact energy. Cs concentrations derived via the sputter yield relation are shown in the inset of

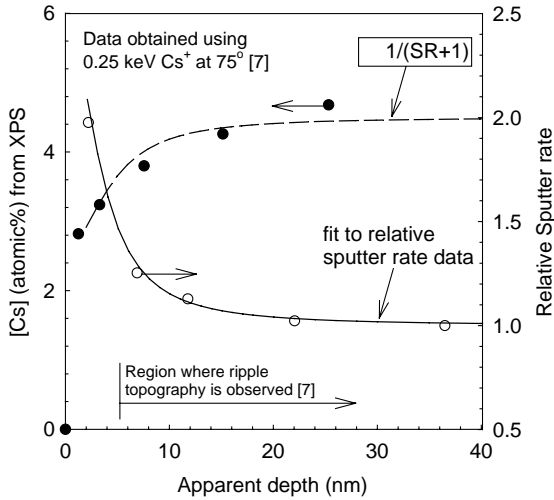


Fig. 2. Cs concentrations derived via XPS and the sputter yield relation from data obtained under conditions resulting in sputter rate variations. The XPS concentrations and relative sputter rates (that normalized to unity) were obtained elsewhere [7].

Fig. 1(b) using simulated and experimentally derived [6] sputter yields. Although only two experimental data points exist, they do exhibit the same trend as those derived from TRIM simulations, i.e., a decreasing Cs concentration with increasing impact energies is noted. This trend is contrary to that observed from XPS and RBS.

Cs concentrations derived from the sputter yield relation under conditions in which excessive sputter rate variations occur as a function of sputtering time (a result of surface roughening as illustrated elsewhere [6,7]) were also derived. These are shown in Fig. 2. The sputter rates and Cs concentrations resulting from 250 eV Cs^+ incident at 75° were obtained in a previous study [7]. The solid line represents a fit to the sputter rate variations, while the dashed line represents the Cs concentration based on the sputter yield relation.

4. Discussion

With the exception of the data shown in Fig. 1(b), the sputter yield relation ($\Delta[\text{Cs}] \propto 1/(\Delta\text{SY} + 1)$) appears to be consistent with the Cs concentration variations noted in this study. The glaring exception concerns the data collected as a function of impact

energy. This shows the XPS and RBS derived Cs concentrations to increase with increasing Cs^+ energy, while Cs concentrations derived from the sputter yield relation decrease. The fact that data from XPS (this relays an concentration averaged over the first ~ 4.2 nm) and RBS (this relays the overall dose) both agree suggests that this is not an artifact of either technique. The increased Cs^+ range at higher impact energies also serves to reduce the uncertainty concerning the analysis depth of XPS, i.e., a more uniform distribution with depth results. Note: both XPS and RBS are used in a retrospective manner, i.e., following sputtering. As a result, the possibility of Cs^+ evaporation from these surfaces during sputtering, if apparent, cannot be examined.

Other factors that may affect the retention of Cs in Si that are not considered by the sputter yield relation include variations in Cs^+ scattering and Cs self-sputtering. Simulations of the scattering coefficient carried out using MARLOWE reveal increasing Cs^+ scattering with decreasing impact energy and increasing incidence angle. These results shown in Fig. 3 are further enhanced as Cs is incorporated onto the Si surface. This is illustrated in the inset of Fig. 3. Simulations also reveal that Cs self-sputtering

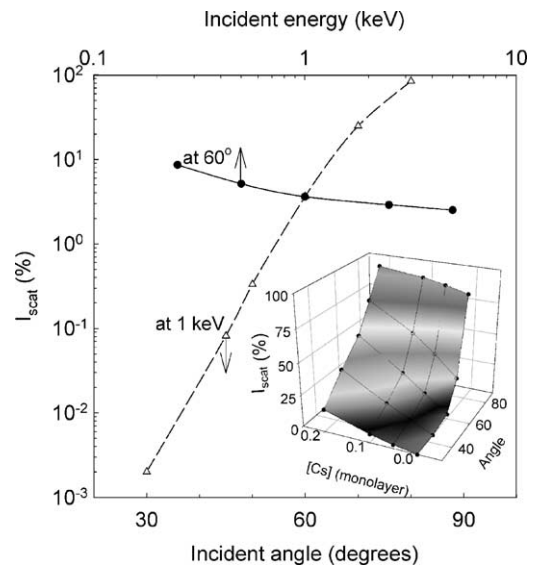


Fig. 3. MARLOWE simulations of the scattering coefficient of Cs^+ primary ions, I_{scatt} , as a function of impact angle (energy fixed at 1 keV) and incident energy (angle fixed at 60°). In the inset is shown how these vary with increasing Cs coverage.

increases with respect to that of Si as the incident energy is decreased [8]. If either or both of these effects become significant, they will reduce the Cs concentration below that implied by the sputter yield relation. This may explain the inconsistent results shown in Fig. 1(b). If so, this will also contribute to the trends illustrated in Fig. 1(a). The inclusion of these effects will therefore be expected to improve the applicability of the sputter yield relation.

5. Conclusions

In general, the $\Delta[\text{Cs}] \propto 1/(\Delta\text{SY} + 1)$ relation appears to describe the variations in the concentration of Cs retained in Si during the sputtering with Cs^+ but only under conditions where scattering and/or self-sputtering are not significant. Cs^+ scattering and self-sputtering are seen to increase with decreasing pri-

mary ion impact energy and increasing incidence angle.

References

- [1] Z.L. Liao, J.W. Mayer, W.L. Brown, J.M. Poate, *J. Appl. Phys.* 49 (1978) 5295.
- [2] V.R. Deline, W. Katz, C.A. Evans Jr., P. Williams, *Appl. Phys. Lett.* 33 (1978) 830.
- [3] J.E. Chelgren, V.R. Deline, W. Katz, C.A. Evans Jr., *J. Vac. Sci. Technol.* 16 (1979) 324.
- [4] D.F. Mitchell, K.B. Clark, J.A. Bardwell, W.N. Lennard, G.R. Massoumi, I.V. Mitchell, *SIA* 21 (1994) 44.
- [5] M.T. Robinson, I.M. Torrens, *Phys. Rev. B* 9 (1974) 5008.
- [6] P.A.W. van der Heide, M.S. Lim, S.S. Perry, J. Bennett, *Nucl. Instrum. Methods Phys. Res. B* 201 (2003) 413.
- [7] P.A.W. van der Heide, M.S. Lim, S.S. Perry, J. Bennett, *Appl. Surf. Sci.* 203–204 (2003) 156.
- [8] W. Eckstein, M. Hou, V.I. Shulga, *Nucl. Instrum. Methods Phys. Res. B* 119 (1996) 477.